

A BESPOKE NON-INVASIVE CURRENT DISTRIBUTION SENSOR FOR USE WITH A FLAT TRANSMISSION LINE

K. Omar, N. Graneau

Hydrodynamics Department, AWE, Aldermaston, Reading, RG7 4PR, UK

B. M. Novac, I. R. Smith

School of Electronic, Electrical and Systems Engineering, Loughborough University, Loughborough, Leicestershire LE11 3UE, UK

Abstract

A determination of the current distribution in a flat transmission line is needed in order to confirm the uniform acceleration of the flyer plate. To this end a novel mutual inductance based sensor has been developed and termed MIDOT.

The sensor is calibrated using a stripline analogue comprised of an array of independent parallel filaments across the width of the transmission line with a known current flowing through each. This enables the positional sensitivity of the sensor to be established. A subsequent series of detailed experiments confirmed that the MIDOT sensor can also be used to identify accurately the currents flowing in the independent filaments under transient conditions.

The sensor has been developed to a stage where its proof of principle has been convincingly demonstrated on a low voltage test bed and it has already been used to provide initial results when fielded on high current facilities.

I. INTRODUCTION

Previous work published by the authors on electromagnetically accelerated flyer plates covered the development of dedicated experimental facilities as well as the development of both one and two dimensional computer models used to understand the performance of the flyer plate [1]. The one dimensional (1D) model has been used to determine the total electrical performance of the circuit and also allowed the bulk flyer motion to be reliably predicted. It was also crucial in developing the current shaping techniques employed by the two capacitor banks [2]. However this paper focuses on the development of the MIDOT sensor and the theory behind it.

II. MIDOT

A. Overview

One feature of current flowing through any transmission line, or flyer-plate, is that the current density is non-uniform across the cross-section of the conductors. The 2D filamentary model has been used to predict this non-uniform current distribution [1] as well as the filamentary current in various other geometries [3]. However, it is still useful to validate these theoretical predictions experimentally.

The sensor proposed here is termed ‘‘MIDOT’’, as it is related to the mutual inductance (M) and the rate of change of current (dI/dt or ‘I-Dot’) in the circuit (‘Midot’). To enable a direct comparison between the model and the experiment, the conductors used for the sensors need to be of the same size as the filaments defined in the 2D model as seen in Figure 1. The induced ‘‘open-circuit’’ voltages (Mdi/dt) from the sensors are then analysed and compared to the theoretically predicted values.

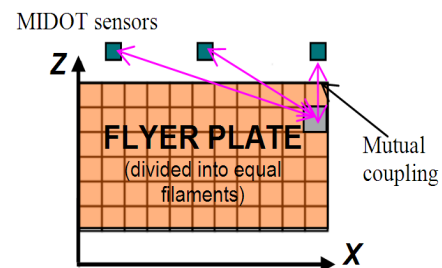


Figure 1, Proposed array of MIDOT sensors installed above the flyer plate. The flyer plate is divided into filaments to allow for the application of the 2D model [1].

B. Single filament tests

An initial experimental arrangement (Figure 2.) was designed to allow controlled low voltage experiments to be carried out. This enabled a better understanding of the mutual coupling between the MIDOT sensor and a single straight wire (filament) before designing more complex experiments. All the wires used throughout the low voltage experiments are 63 μm enamelled copper (known as magnet wire).

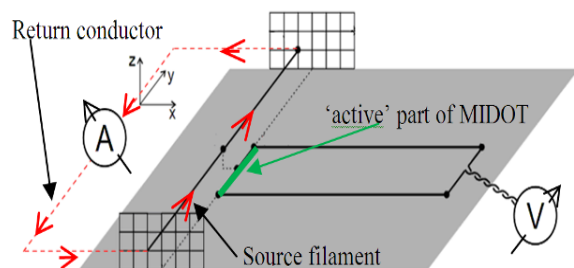


Figure 2, Single filament MIDOT setup.

In the above figure the current source filament is parallel to the MIDOT with the return conductor much further away to reduce its mutual coupling. ‘A’ and ‘V’

are current and voltage monitors respectively. The ‘active’ part of the MIDOT is also indicated.

As the induced signal is directly proportional to the time rate of change of the current, a very fast current pulse is required. This is achieved by using a Stanford pulse generator capable of driving a current pulse with a rise time of ~ 90 ns (in to a 50Ω load) as shown in Figure 3.

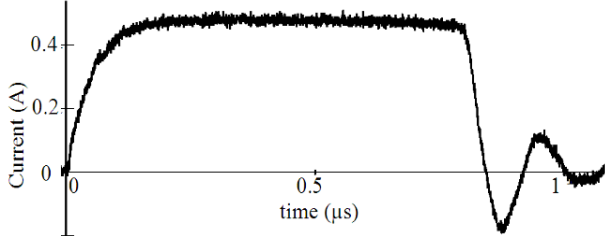


Figure 3, Current pulse from Stanford pulse generator (connected to a 50Ω load) measured using a calibrated Pearson current monitor (‘A’ in Figure 2.).

The induced voltage measured across the MIDOT circuit (Figure 4.) is simply the ‘emf’ ($M di/dt$), where M is the mutual inductance between the MIDOT and the source filament. The induced emf is overwhelmingly dominated by the mutual coupling between the source filament and the active part of the MIDOT circuit with no contribution from the perpendicular wires.

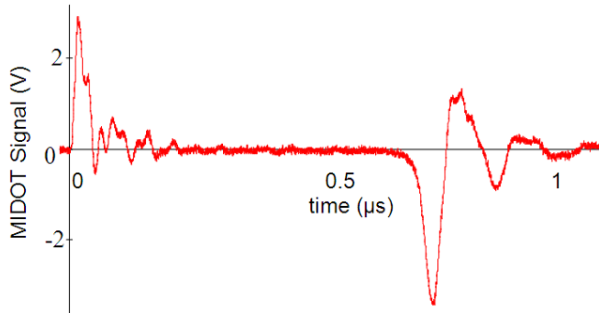


Figure 4, Measured ‘ $M di/dt$ ’ signal from sensor positioned $250 \mu\text{m}$ directly above the source filament.

Equation 1 below represents the measured emf for the MIDOT; this is then numerically integrated as shown in equation 2 to obtain ‘MI’. As ‘ I ’ is already known (from direct measurement, see Figure 3.); the actual mutual inductance for the MIDOT used in the experiment can be determined.

$$V_{MIDOT} = M \frac{dI}{dt}, \quad (1)$$

$$\int V_{MIDOT} = \int M \frac{dI}{dt} = M \int \frac{dI}{dt} = MI, \quad (2)$$

Theoretically the mutual inductance for any pair of straight parallel filaments (i and j) can be calculated using the well-known *exact* formula (equation 3) published by Grover [4]:

$$M_{ij} = \frac{\mu_0 I}{2\pi} \left(\ln \frac{l + \sqrt{l^2 + \text{dist}_{ij}^2}}{\text{dist}_{ij}} - \frac{\sqrt{l^2 + \text{dist}_{ij}^2}}{l} + \frac{\text{dist}_{ij}}{l} \right), \quad (3)$$

where dist_{ij} is the geometrical mean distance (GMD) between the two filaments and l is the length of the ‘active’ part of the MIDOT (Figure 2.).

Varying the separation of the sensor relative to the source filament generates a spatial mutual inductance intensity map which can be used to establish the resolution of the MIDOT. This is shown in Figure 5. for the single source filament experiment. The discrepancy between the model and experiment is due to errors in both the lateral positioning and the height of the MIDOT above the plane of the source current.

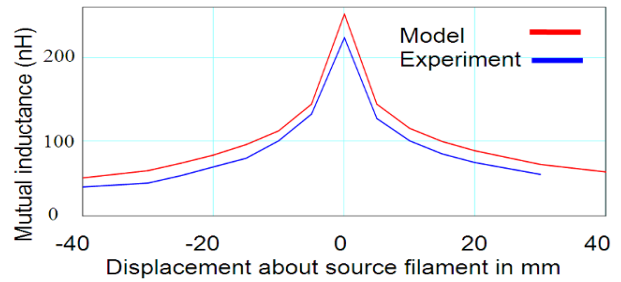
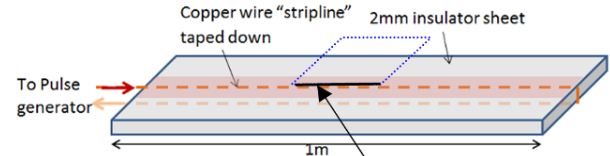


Figure 5, Experimental and modelled mutual inductance coupling across a single source current filament. ‘Zero’ position corresponds to the active part of the MIDOT being directly above the source filament.

C. Transmission line geometry and theoretical predictions

To better represent the flyer plate experiments a stripline (transmission line) arrangement was constructed using the filamentary approach. The top and bottom conductors of the transmission line are now separated by a 2 mm sheet of polyethylene to mirror a realistic flyer plate geometry (Figure 6.). The sensor is kept in the centre of the filament to both reduce the effects due to the ends of the stripline and also to allow equation 3 to be valid. The height of the MIDOT is fixed during construction of the sensor (section III).



MIDOT sensor – separated from stripline by $90 \mu\text{m}$ tape layer.
Figure 6, Transmission line experiment; return path 2 mm directly below top conductor.

Using equation 3 to determine the net mutual inductance for the MIDOT with both the top and bottom conductors immediately highlights the benefit of the new arrangement, as shown in Figure 7.

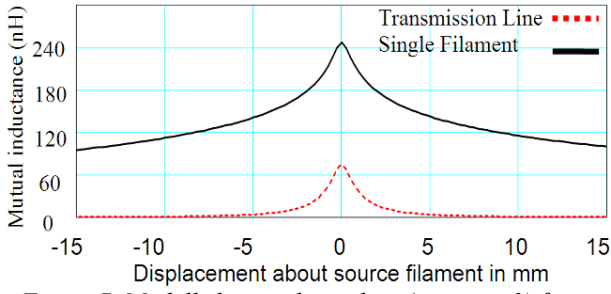


Figure 7, Modelled mutual coupling (equation 3) for a single source filament compared to a 2mm separated stripline arrangement.

Despite a lower net signal, the transmission line arrangement gives more localised mutual coupling which quickly drops to zero with lateral distance from the source current. In this particular configuration the MIDOT is only sensitive to current flowing 2-3 mm either side of it. Whereas the single filament arrangement still has a strong mutual coupling to the source current even if placed 15mm away.

D. Transmission line experiments

The induced voltage from the stripline geometry is shown in Figure 8a; the two signals captured are by connecting the high impedance probe to either side of the MIDOT circuit (this has been defined as the positive and negative polarity of the MIDOT).

When the probe is connected to the MIDOT it creates an asymmetric circuit with the high impedance load on one side. By ‘reversing the polarity’, the high impedance is put on the opposite side of the circuit. Processing these two signals allows the effect of the loading to be removed.

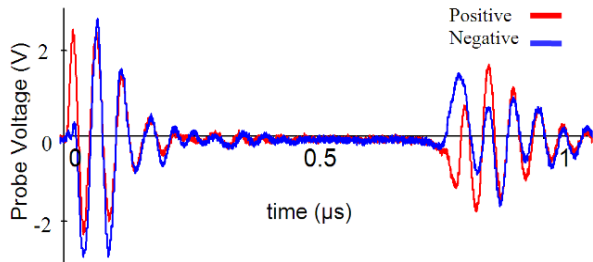


Figure 8a, Raw MIDOT signals (positive and negative) from the stripline.

$$V_{MIDOT}^{\pm} = \pm M \frac{dI}{dt} + \frac{Q}{C} + (noise), \quad (4)$$

Subtracting the ‘negative’ signal from the ‘positive’ and dividing by two removes any capacitive components as well as any noise and ringing due to the asymmetrical loading of the MIDOT circuit. This leads to the better quality signal, as shown in Figure 8b. This procedure is equivalent to using a high impedance differential probe.

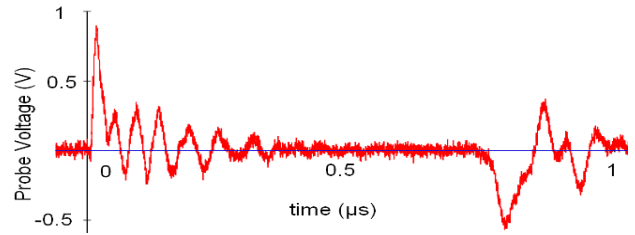


Figure 8b, Processed MIDOT signal from the stripline arrangement.

Integrating the processed signal (Figure 8b.) allows the mutual inductance to be determined. The modelled and measured results for a range of separations are shown in Figure 9.

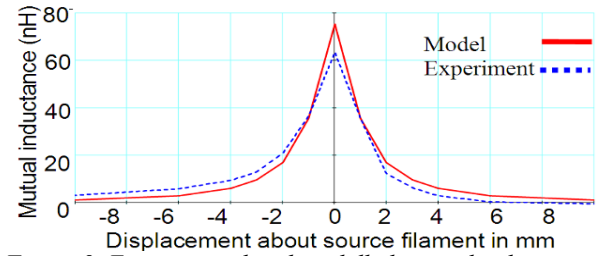


Figure 9, Experimental and modelled mutual inductance coupling for stripline geometry.

Comparing Figure 9. to Figure 5. confirms the improvement in the sensitivity of the MIDOT. It also shows that it would be possible to position a series of MIDOTS ~4mm apart to determine the current flow across the stripline in 4m strips.

III. MIDOT ARRAY

A. Array development

An array of MIDOT sensors allows data from across a stripline to be obtained without having to move the actual equipment, ensuring consistency between shots. Comparing the results from the single MIDOT scan and equivalent data from the array confirmed that the presence of multiple sensors does not affect the results. This is a consequence of the extremely low current (μA) flowing through the sensors which are terminated with high impedance voltage probes.

The array was constructed by fixing the MIDOT filaments into channels machined in a polycarbonate sheet (the channels were 500 μm wide and 500 μm deep, with the adjacent channels 2mm apart) as seen in Figure 10.

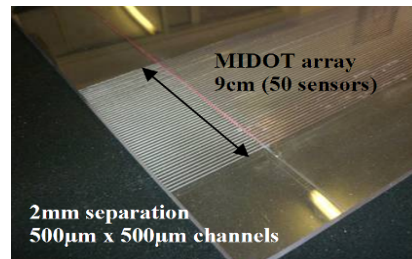


Figure 10, Completed MIDOT sensor array.

A schematic of the array is shown in Figure 11. The vertical sections of each loop run in a single (wider) channel; as the wire used is enamelled this keeps all the loops electrically isolated.

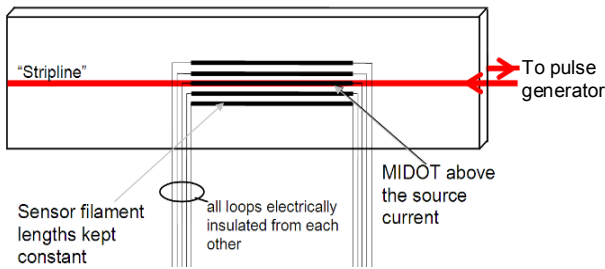


Figure 11, MIDOT array positioning for single filament test.

Figure 12 shows how the induced voltage measured on adjacent sensors varies for the same source current using the MIDOT array.

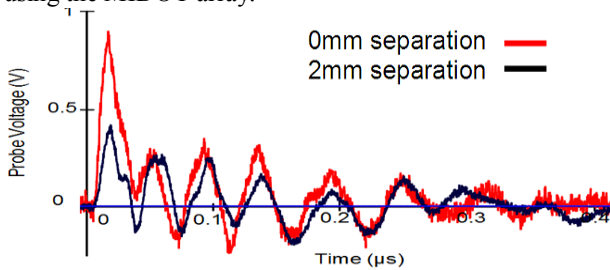


Figure 12, Processed MIDOT signals for '0 mm' and '2 mm' separation. This clearly shows the reduction in the induced voltage.

Integrating the above signals provides good agreement with Figure 9; proving there is no effect on the system due to the large number of parallel sensors.

The MIDOT sensor is also very sensitive to its vertical position and even a difference of a few hundred microns in the distance between the MIDOT plane and the source filament plane (which is fixed during the array construction) can cause a noticeable variation in performance as shown in Figure 13.

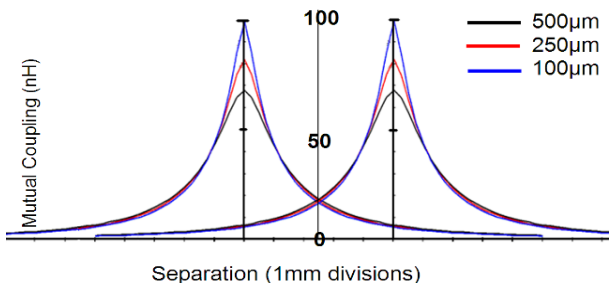


Figure 13, MIDOT coupling for three different channel depths.

As expected, the closer the sensor is to the current source, the stronger the coupling. Figure 13. also indicates that it is possible to easily distinguish 2 separate current sources even if they are only 2 mm apart using the array.

B. MIDOT calibration

Passing a known current pulse under each sensor in the array and recording the induced voltage allows the array to be calibrated i.e. determine the actual mutual inductance for each MIDOT sensor in the array. An error of $\pm 10\text{nH}$ in the mutual coupling of the MIDOT to the source filament is found due to errors in the vertical positioning of the MIDOT during construction.

The peak signal for each MIDOT is measured by positioning the sensor directly above the stripline (i.e. the "zero position"). Using the geometry outlined in Figure 14. together with equation 3 allows the theoretical value to be calculated; comparing this to the measured MIDOT coupling gives the results in Figure 15.

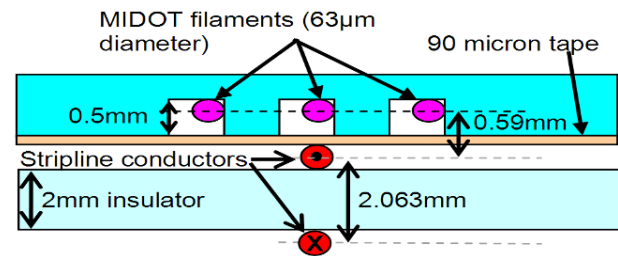


Figure 14, MIDOT and stripline schematic, (not to scale).

The modelled mutual coupling for the experimental arrangement is 59.15 nH. The actual measured values are shown in Figure 15.

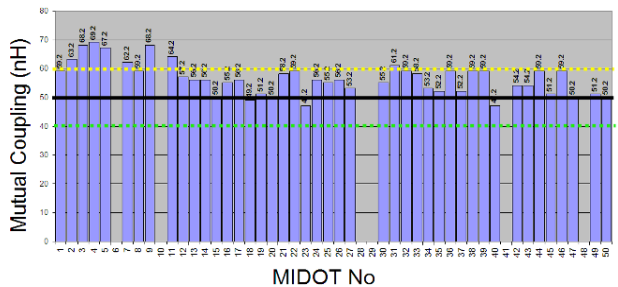


Figure 15, Measured mutual coupling for each MIDOT.

As seen in Figure 15, the majority of deviations from the model are within the expected positional error indicated by the dotted lines above and below the modelled value.

Due to the width of the machined channel, the lateral position of the MIDOT can only be known to \pm half the channel width. This adds an additional lateral positioning error of $\pm 7\text{ nH}$ (independent of the vertical height errors shown in Figure 15.). This can only be reduced by constructing a new array with narrower channels.

C. Dual filament tests

The following tests were designed to assess the capability of the array to initially resolve two separate current sources. To represent the 9 cm wide stripline as used on AMPERE [1, 2], 17 individual source filaments were assembled, spaced 5 mm apart (Figure 16.) and

independently connected to the Stanford signal generator.

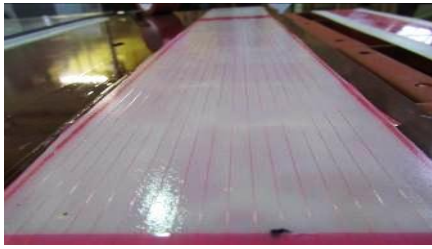


Figure 16, Filamentary analogue of flat transmission line.

Each of the Stanford rear ('HV') outputs are capable of driving up to 800 mA into a 50 Ω load. They can also be simultaneously triggered allowing for multiple current pulses (Figure 17.).

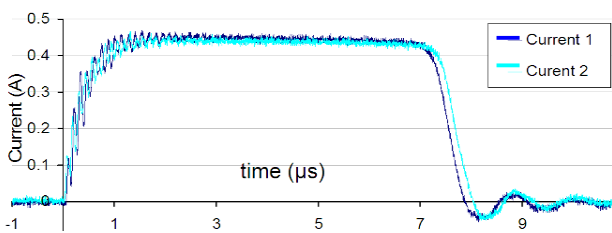


Figure 17, Two independent current pulses simultaneously triggered from the Stanford generator.

Initially, two independent source filaments with a large lateral separation (4cm) were used (see Figure 18.).

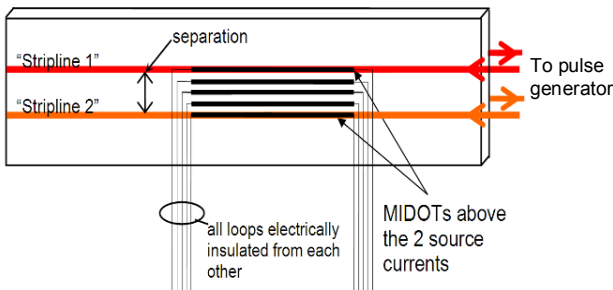


Figure 18, Dual source filament test schematic.

Measurements are taken across the entire MIDOT array. The voltage from each MIDOT is first 'cleaned' using the technique outlined in section II and then integrated. All the integrated traces are plotted on the same set of axes. Only the MIDOT closest to the source current will produce a large integrated trace. This, coupled with the calibration of the MIDOT array (Figure 15.), allows the actual source current to be determined for each of the identified sensors.

Figure 19. shows the processed data. For clarity, only the two peak signals and a couple of adjacent traces are plotted.

Figure 20. shows the actual current levels determined using the calibrated sensor. Errors in the lateral positioning of the MIDOT sensors allow MIDOT(min) and MIDOT(max) to be obtained.

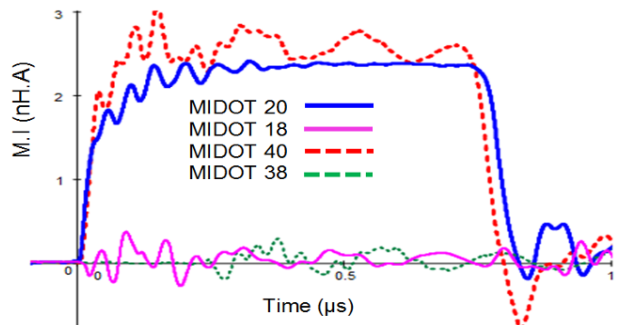


Figure 19, Processed MIDOT data, MIDOTs 20 and 40 clearly identified as closest to the source filaments.

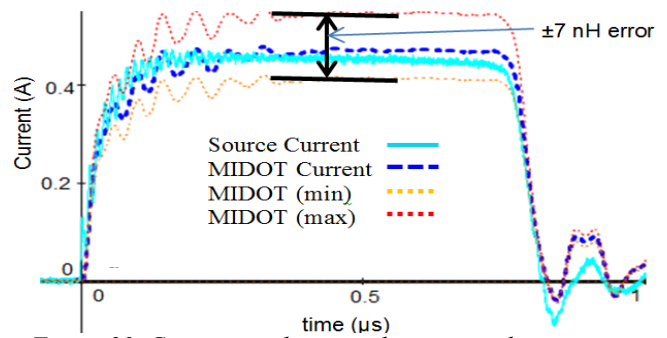


Figure 20, Comparison between the measured current pulse and the current determined from MIDOT 20.

The MIDOT current is in very good agreement with the measured source current. Results for MIDOT 40 also agree with the measured current to within experimental errors.

It is clear to see that the MIDOT technique can clearly determine the location of and also the absolute value of independent source current filaments in the low voltage experiments.

D. Competing techniques described in the literature and the advantage of using MIDOT arrays.

Techniques to determine the current distributions have been published previously [5]; one of the more recent approaches has been to use the Colossal Magneto Resistive (CMR) effect of specific materials [6]. The major drawback of this technique is that a dedicated complex computer model is necessary to determine the current distribution required, to generate the magnetic field causing the measured effect. It is also possible for a number of different current distributions to generate the same total magnetic field at a particular location. Another important factor that cannot be neglected is the cost of the probes: a single CMR probe is much more expensive than all the filaments utilised in a MIDOT array!

The benefit of the MIDOT approach is that a direct and localised measurement of the current (or immediate effect of the presence of current) is obtained. Almost no computation is necessary to understand the results and the MIDOT could also be used to validate a 2D code.

Due to the design of the MIDOT sensor, it

automatically integrates the measurement along the whole length of the sensor. This in effect reduces the problem to 2D. The CMR probes provide sufficient localisation but are only 500 μm long and so require a large number of sensors positioned along the length of the flyer during a single shot to obtain data equivalent to that obtained from a MIDOT array during a single shot.

E. Initial high current tests

Experiments were carried out on the Quattro bank at Loughborough [7] using 2 MIDOT filaments which were 50 μm thick and 2.5mm wide (the closest match to the filament size in the 2D model described in [1]) as shown in Figure 21.

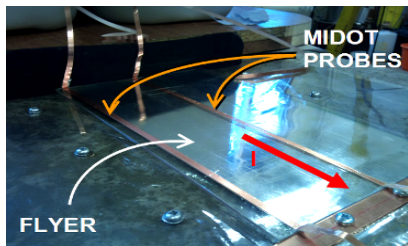


Figure 21, MIDOT sensors positioned above flyer plate section on Quattro.

Placing one sensor in the centre of the flyer and another along the edge allowed the largest difference in signals to be measured. Figure 22. shows the current pulse during a Quattro discharge and the associated MIDOT data compared with prediction from the 2D model is shown in Figure 23.

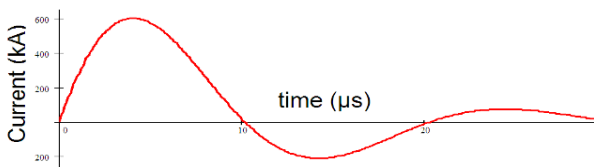


Figure 22, Typical current impulse generated by Quattro.

Figure 23. is a comparison of the modelled and measured voltage for the probe at the edge of the flyer.

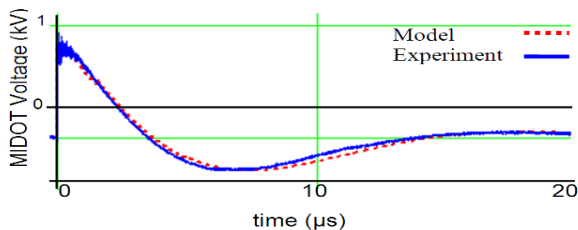


Figure 23, 2D theoretical predictions compared with experimental data for a MIDOT placed 250 μm above the flyer.

The results from these experiments show that a MIDOT sensor generates data that can be used to better understand the transient current flow in a transmission line. A large series of tests using a dedicated experimental rig are about

to be conducted to further develop the understanding of the MIDOT array sensor fielded in high current systems.

IV. CONCLUSIONS AND THE WAY AHEAD

A novel type of sensor termed MIDOT has been invented, designed, manufactured and successfully tested on both low and high current systems. A MIDOT sensor, which only uses straight very thin wire, can produce an open circuit signal proportional to the current in an adjacent conductor. Even more, the MIDOT appears to be so sensitive as to identify the position of a pair of transmission line conductors with a precision better than ± 2 mm. Using these two properties, a MIDOT array can be used to easily determine the time-variation of the current distribution in a parallel-plate transmission line.

Further work is already planned to be conducted on the MIDOT technique using a specially constructed high-current rig. One benefit of moving to a higher current will be that the noise and capacitive stray effects associated with the low current results presented in this paper will be much reduced so that their analysis will become much easier.

Finally, MIDOT arrays will be used on the AMPERE and Quattro facilities to probe the time varying current distribution during a flying plate shot.

V. References

- [1] B. Novac, et al, "Numerical modelling of a flyer plate Electromagnetic Accelerator," IEEE Trans. on Plasma Science, 40(10), pp. 2300-2311, Oct 2012.
- [2] K. Omar et al, "FOIL-FLYER Electro-Magnetic Accelerator, Initial Results From A New AWE Pulsed Power Generator," 18th IEEE Int. Pulsed Power Conference, Chicago, IL, USA. 2011.
- [3] C. Mielke and B.M. Novac, "Experimental and Numerical Studies of Megagauss Magnetic Field Generation at LANL-NHMFL," IEEE Trans on Plasma Science, 38(8), pp. 1739-1749, 2010.
- [4] F.W. Grover, Inductance Calculations. Working Formulas and Tables, Dover Publications, Inc., New York, 1946.
- [5] O. Leibfried et al, "Measurement of the Magnetic field Distribution in railguns using CMR-B Scalar sensors," in proc. ACTA physica Polonica A, Vol 115. (2009), pp1125-1127.
- [6] S. Balevicius et el, "High frequency CMR-B Scalar sensor for Pulsed Magnetic field Measurements," 4th EAPPC, Karlsruhe, Germany, 2012
- [7] K. Omar et al, "Flyer Plate Electromagnetic Accelerator Modelling and Development of Bespoke Sensor Technology," presented at 14th Int. Conf. Megagauss Magnetic Field Generation and Related Topics, Maui, Hawaii, 2012.